The Effect of Swirl on Spark-Ignition Engine Combustion

Y. Hamamoto, E. Tomita, Y. Tanaka and T. Katayama,
School of Engineering, Okayama University.
Tsushima-Naka 3, Okayama, 700

ABSTRACT

In order to investigate the effect of swirl on combustion in a spark-ignition engine, a new experimental apparatus was developed. The test engine has a 78 mm bore, an 85 mm stroke and a pancake type combustion chamber. In this engine, the combustion phenomena in various intensity of swirl flow can be investigated. The swirl flow in the cylinder was visualized by a smoke-wire method, and a laser Doppler anemometer and a hot-wire anemometer were adopted for the measurement of the velocity. The turbulence intensity was determined on the basis of the hot-wire data. Stoichiometric propane - air mixture was ignited at the center of combustion chamber. The effect of swirl on combustion in cylinder was investigated under various conditions of compression ratio and engine speed. As a result, it was found that the burn duration could be expressed as a function of the turbulence intensity. The effects of engine speed and the swirl ratio are not explicit and are included implicitly in the term of turbulence intensity.

INTRODUCTION

It is well known that the turbulent flow field in a spark-ignition engine cylinder plays an important role in determining the characteristics of combustion, thermal efficiency and exhaust emissions(1). For reducing the level of NOx emissions, EGR (exhaust gas recirculation) is effective, and the use of lean mixture improves the thermal efficiency of the engine. The use of lean mixture or EGR, however, causes the cycle-to-cycle fluctuation of combustion and the deterioration of driveability.

In spark-ignition engines, faster burning can raise thermal efficiency and reduce NOx emissions by extending the range of stable engine operation, allowing very dilute fuel/air mixtures to be used(2). It is an important theme that the influence of turbulence and mean fluid motion on combustion is made clear and that a model describing these interactions is developed(3).

The entrainment eddy burning model seems a reasonable phenomenological model(4-7) for turbulent combustion in the spark-ignition engine. For further development of this combustion model, it is necessary to make clear the turbulence characteristics and the interaction between turbulence and combustion in the engine cylinder.

In this study, to reveal the effect of turbulent swirl on combustion, a new experimental engine was prepared. The mixture of propane and air is ignited at the center of pancake type combustion chamber. Thus, the flame propagates in the flow field of various intensity of swirl accompanied with no squish flow. Namely, the combustion seems to progress in relatively simple manner.

As the first step in a series of the turbulent combustion research in the spark-ignition engine, presented in this paper are the detail of the experimental apparatus, the measurements in the turbulent swirl and the effect of turbulence intensity on burn rate and burn duration.

EXPERIMENTAL APPARATUS

In order to reveal the effect of swirl on combustion in a spark-ignition engine, a new experimental apparatus was developed. Figure 1 shows a schematic diagram of experimental apparatus, and Table 1 shows main dimensions of this test engine and experimental conditions.

The engine cylinder and the mixture tank are connected with each other by a pipe. When the engine is driven by an electric motor, the fuel gas (propane) and air go back and forward between the cylinder and the tank through the intake valve which is normally opened, and fuel gas and air are mixed homogeniously. After making preparation for homogeneous mixture in this way, the intake valve is closed at BDC, and then the mixture in the cylinder is compressed and expanded repeatedly by the piston motion.

During the intake stroke, the swirl flow is produced in the cylinder. The combustion chamber is pancake type, therefore no squish flow is produced. The swirl velocity at TDC of compression stroke decreases with the increase of the number of compression stroke, N, after the valve close. By igniting the mixture near end of compression in various number of compression stroke after the valve close, the combustion phenomena in various intensity of swirl flow can be examined.

It is possible, in this test engine, that the flow pattern in the cylinder is visualized. The test engine has an elongated piston with a glass crown. By providing a slot in the side of the elongated piston, an inclined mirror inside the piston could be fixed to the cylinder block. The

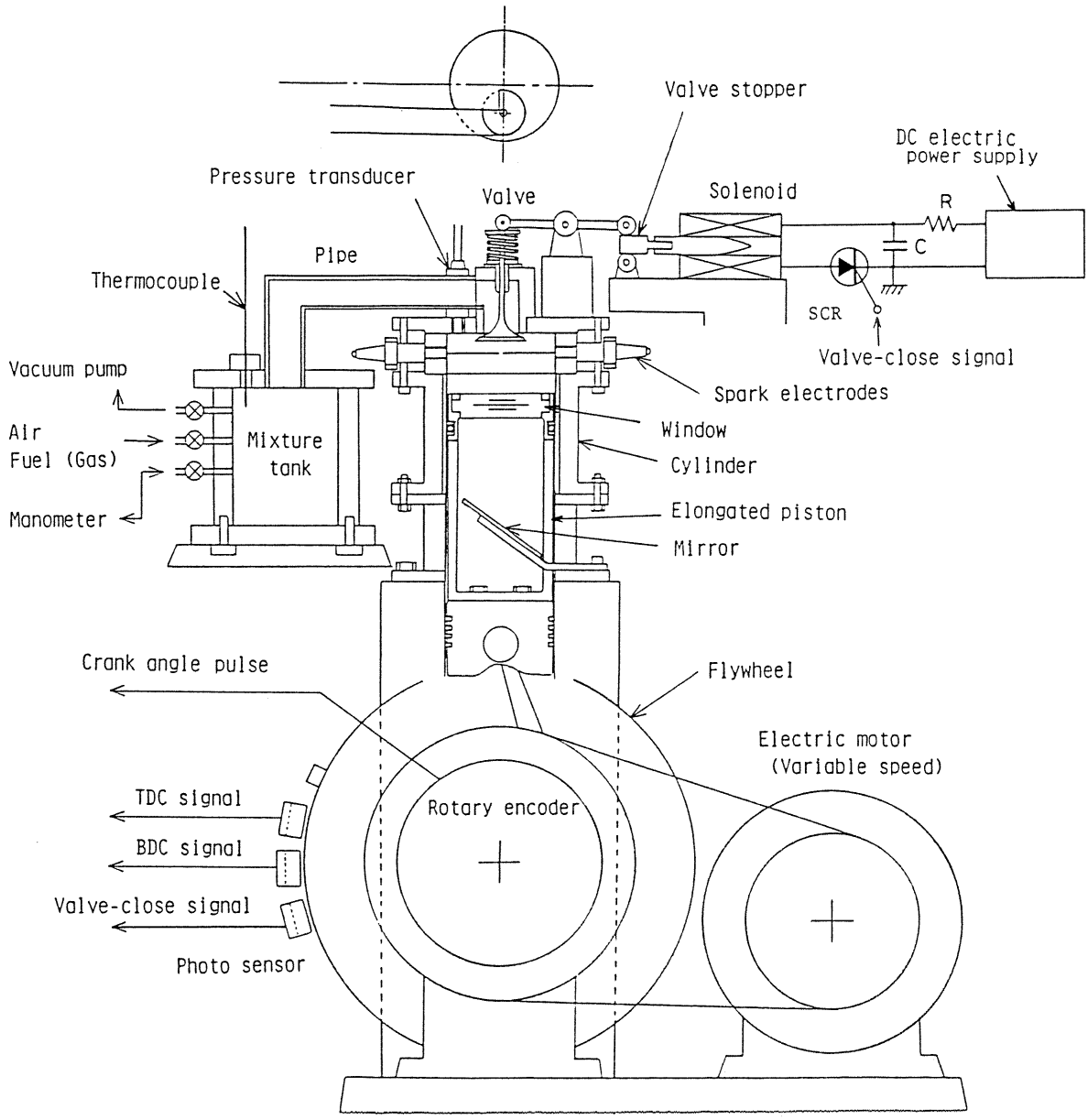

Fig.1 Schematic diagram of experimental apparatus

Table 1. Main dimensions of test engine and experimental conditions

Cylinder diameter	78 mm
Stroke	85 mm
Length of connecting rod	153 mm
Compression ratio	3.2, 4.0, 4.8
Combustion chamber	Pancake type
Fuel	C_3H_8
Equivalence ratio,	1.0
Engine speed	600, 900, 1200 rpm

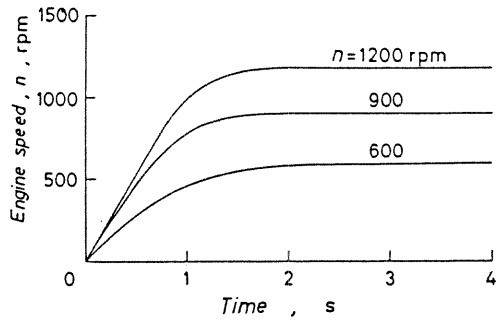

Fig.2 Change of engine speed after start

gastightness in the cylinder is kept by using a rubber o-ring instead of ordinary piston rings. The spark gap for ignition is located in the center of combustion chamber in the midplane of the clearance volume.

Operations of the experimental apparatus are controlled by a computer. Top dead center (TDC), bottom dead ceter (BDC) and valve-close signals are produced with photo-sensors, and a pulse train of crank angle is produced by an electromagnetic rotary encoder (360 pulses/rev.).

When the valve-close signal is added to the SCR-circuit in accordance with the computer command, the electric discharge occurs through the solenid coil. Then, the stopper piece is removed and the valve closes by the force of spring. The time interval between the valve-close signal and the actual valve close is 5.04 msec. Consequently, for making the valve to close at the BDC, it is necessary that the valve-close signal is added to the SCR-circuit at 5.04 msec. before the BDC.

The change of engine speed after the start was investigated. As shown in Fig.2, the engine speed in steady state are attained in shorter time than three sec. In this test engine, the mixture of propane and air is prepared by going and returning between the cylinder and the tank. The homogenization of mixture was attained at about fifty revolutions of the engine.

The amount of the mixture in the cylinder after the valve close was estimated from the measurements of temperature and pressure in the cylinder and the mixture tank. The results was shown in Fig.3. In the range of experimental conditions, the mass of the cylinder charge varies with compression ratio, ε, and hardly depends on the engine speed, n.

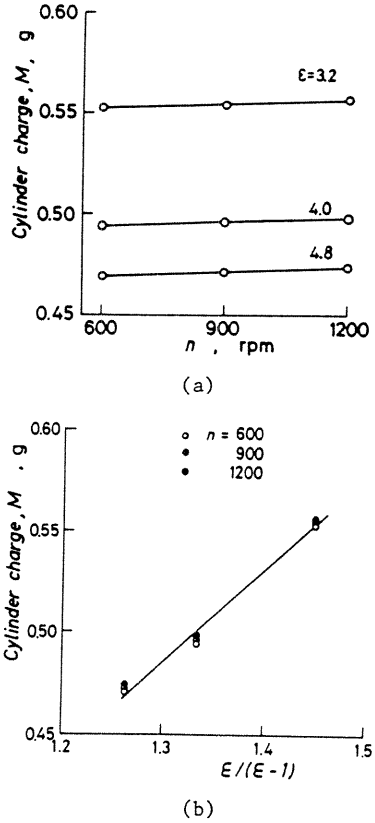

Fig.3 Amount of mixture in cylinder after valve close

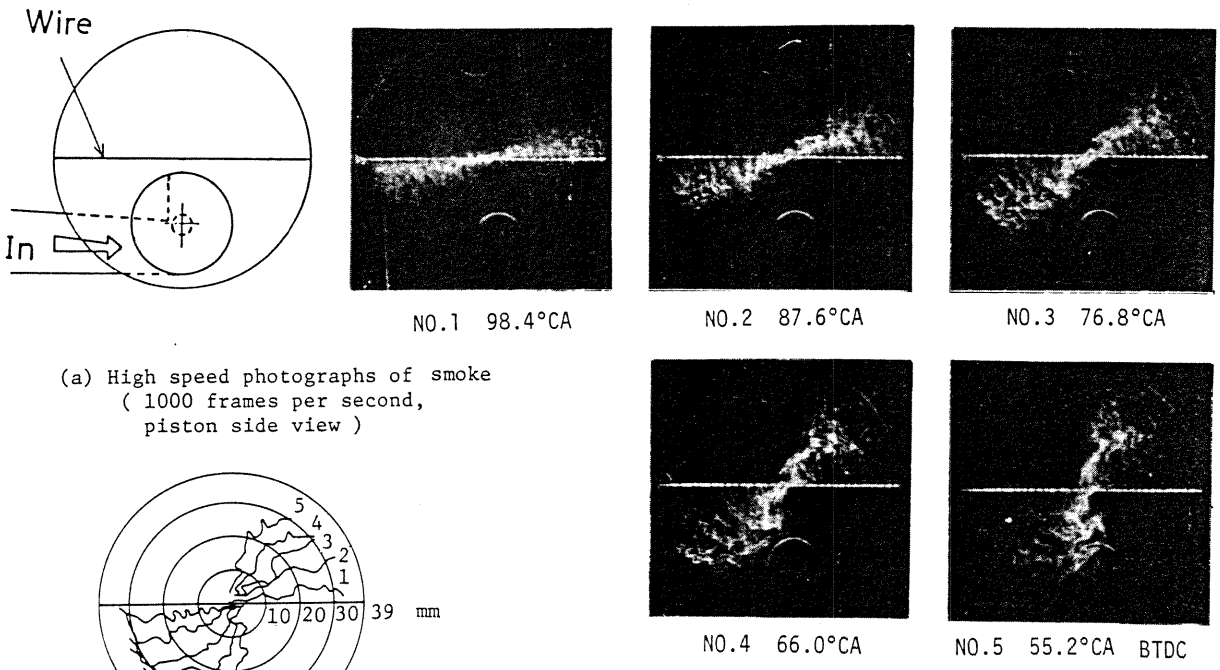

(a) High speed photographs of smoke (1000 frames per second, piston side view)

(b) Overlapped tracing of the smoke front

Fig.4 Visualization of air swirl in cylinder by the smoke-wire method
(ε = 4.8, n = 600 rpm, N3)

SWIRL FLOW IN CYLINDER

Flow Visualization in Cylinder by Smoke-Wire Method

By applying a smoke-wire method(8), the air swirl in the cylinder was visualized for the case of non-combustion. The resistance wire (nickel) coated with oil (glycerin) was set up in the cylinder. The oil was vaporized by heating the wire electrically in the predetermined crank angle, and then the oil vapor was cooled by ambient air and the white oil mist (smoke) was formed.

Two nickel wires each being 0.2 mm in diameter were intertwisted and set up in the midplane of the clearance volume and in the direction of the cylinder diameter. This cylinder part was made transparent, and the smoke was illuminated from the flank and taken photograph from below the piston using a reflex mirror and a high speed camera. An electric current for heating the smoke-wire was supplied from the discharge condenser which the capacity was 2500 μF and the charging voltage was 75 V.

Figure 4 shows an example of visualization of air swirl by the smoke-wire method (SW). It is the air swirl during the third compression stroke after the valve close (N3) at the engine speed, n, of 600 rpm and the compression ratio, ε, of 4.8. Figure 4(b) shows the overlapped tracing of the smoke front. The angular velocity of characteristic points of the smoke front to the cylinder axis was measured, and the swirl velocity in the tangential direction was determined. The tangential velocity distribution along the cylinder radius is shown in Fig.5, where $\bar{U}$ and r denote the mean velocity in crank angle interval between 110 and 55 degrees BTDC and the distance from the cylinder axis, respectively. It is recognized from these results that the swirl flow in the cylinder during compression stroke was similar to a solid body rotation in velocity distribution. The figure also shows the results of measurements made by a laser Doppler anemometer (LDA) and a hot-wire amemometer (HWA). These results measured by three kinds of methods, SW, HWA and LDA, almost agreed with each other.

It is one of the problems of the smoke-wire method that the smoke disappears when the air temperature becomes high. Consequently, the air swirl near TDC could not be visualized.

Mean Velocity and Turbulence Intensity of Swirl Flow in Cylinder

The flow velocity of swirl in cylinder after the valve close was measured by using a constant temperature type hot-wire anemometer(HWA) and a laser Doppler anemometer (LDA). The velocity measurements were made on a line in the midplane of clearance volume, as shown in Fig.6.

A HWA has good characteristics in the frequency response and is effective for the measurement of turbulence. However, it is also sensitive to temperature and pressure of the air stream. Therefore, there is a serious problem in hot-wire anemometry in an engine cylinder, where temperature and pressure of gas change rapidly in wide range. In particular, the exact determination of the gas temperature near TDC is very difficult. In order to eliminate the uncertainty of hot-wire anemometry of the velocity near TDC, in this study, the values of mean velocity measured with the HWA were confirmed by the LDA.

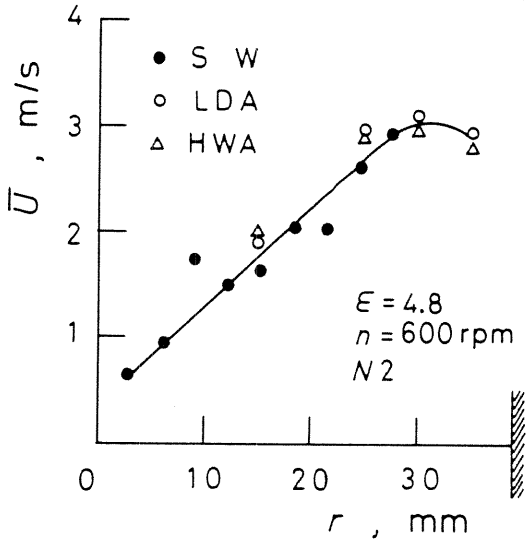

Fig.5 Comparison of the mean velocities with three kinds of measuring methods (SW, LDA, HWA)

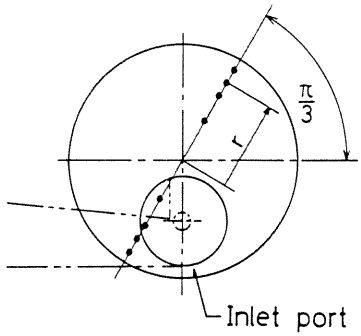

Fig.6 Location of measuring point of velocity (midplane of the clearance volume)

The sensing element of a HWA used in this study was made of platinum-iridium alloy, and its diameter and length were 15 μm and 2 mm, respectively. The temperature of wire was kept constant at 800 K. It was recognized by using a spark tuft method(9) that the swirl flow near TDC was almost horizontal. Therefore, the sensing element of a HWA was set in the parallel direction to the cylinder axis. For the changes of gas temperature and pressure and the conductive heat loss to the wire supports, the output of a HWA was compensated(10) as described in Appendix A.

Figure 7 shows the optical arrangement of the LDA system. The LDA operated in the fringe mode of forward scattering type and incorporated with a frequency shifter of Bragg cell type. The light source was helium-neon laser of 15 mW, and the wave length was 632.8 nm. The total angle of intersection of laser beams was 0.2023 radians (11.59 degrees). The length of intersection region was about 1.14 mm and the diameter was about 0.12 mm. JIS test dust No.11(fine red clay) was used as particles for scattering the light. The Doppler signals were processed with a frequency tracking system.

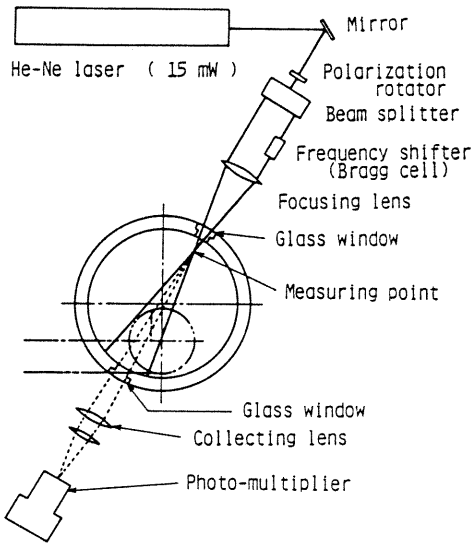

Fig.7 Optical arrangement of LDA system

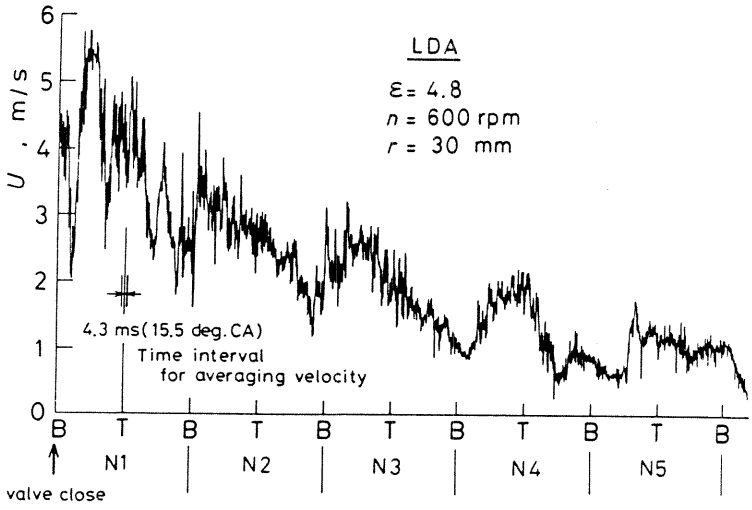

Fig.8 Example of swirl measurement with LDA (n = 600 rpm, ε = 4.8, r = 30 mm)

Figure 8 shows an example of the tangential velocity of swirl flow, U, measured with the LDA. The measurement was made for the case with compression ratio ε=4.8, engine speed n= 600 rpm and the location of measuring point r=30 mm. It is recognized that the swirl velocity near TDC decreases with the number of compression stroke after the valve close, N.

In this study, the mean velocity, $\overline{U}$, and the intensity of turbulence, u', near TDC were defined in accordance with the stationary time-average method which treated the flow in a given short time interval from TDC - Δt/2 to TDC + Δt/2 as a steady flow(11). Namely,

instantaneous velocity in the k-th run of experiment:

U_k,

mean velocity in the k-th run of experiment:

$$\overline{U}_k = \frac{1}{\Delta t}\int_{-\Delta t/2}^{\Delta t/2} U_k \, dt \quad ,$$

fluctuating component of velocity in the k-th run of experiment:

$$u_k = U_k - \overline{U}_k \quad ,$$

mean velocity:

$$\overline{U} = \frac{1}{Z}\sum_{k=1}^{Z} \overline{U}_k \quad ,$$

turbulence intensity:

$$u' = \sqrt{\frac{1}{Z}\sum_{k=1}^{Z} u_k^{\,2}} \quad .$$

(Z is the number of run of experiments; Z=10-20 in the measurement of turbulence intensity.)

The data sampling frequency was 20 kHz in this study. By employing the finite time interval, Δt, the fluctuating component of velocity (turbulence) having lower frequency than about 1/(2Δt) is cutoff(12). The cutoff frequency was about 116 Hz in this study, because Δt was chosen as 4.3 msec. The choice of 116 Hz in the cutoff frequency was based on the report that the turbulence having lower frequency than about 100-150 Hz hardly affects combustion(13).

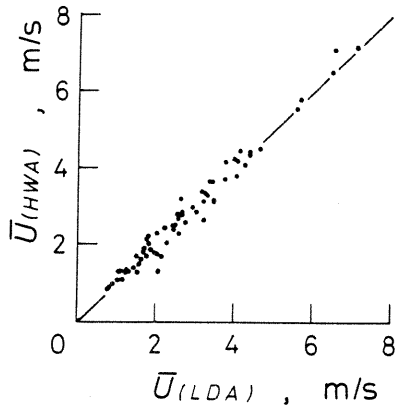

Fig.9 Comparison of mean velocities between HWA and LDA

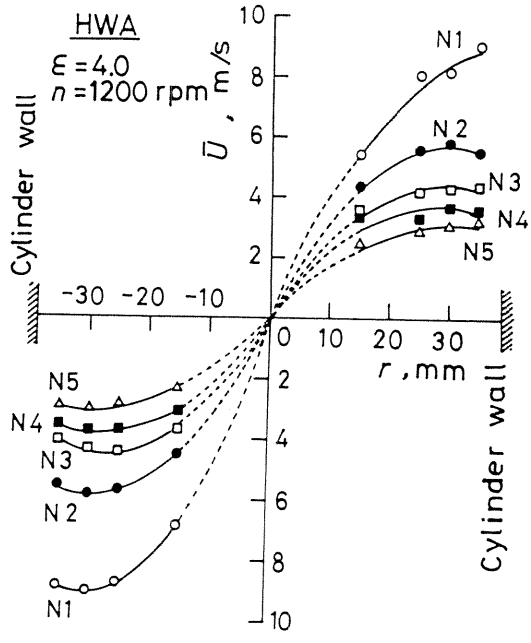

Fig.10 Mean velocity of swirl near TDC (ε = 4.8, n = 1200 rpm)

By using the HWA and the LDA, the measurements of mean velocity near TDC were made in many kinds of experimental conditions, and both results were compared with each other as shown in Fig.9. The measured values with the HWA almost coincided with LDA data. Consequently, it was confirmed that the HWA output was compensated with good accuracy.

Figure 10 shows the mean velocity near TDC determined with HWA for the case with ε=4.0 and n=1200 rpm. The pattern of velocity distribution in this figure was very similar to the results obtained under other conditions of compression ratio and engine speed. From such a velocity distribution curve of swirl, the anguler momentum to the cylinder axis was calculated, and the anguler speed of an equivalent solid body rotation was obtained. In this way, swirl ratio, SR, was defined as a ratio of the speed of equivalent solid body rotation to the engine speed.

The measured values of swirl ratio, SR, mean velocity, $\bar{U}$, and turbulence intensity, u', near TDC are summarized in Table 2. Figure 11 shows the reduction in swirl ratio during the repeat of compression and expansion.

The value of multiplied SR by n, n·SR, is representative speed of swirl flow in cylinder. Then, the values of mean velocity determined at r=30 mm, $\bar{U}$, were compared with n·SR. As a result, it was recognized that a good linear correlation between $\bar{U}$ and n·SR as shown in Fig.12. Consequently, $\bar{U}$ at 30 mm of r could be treated as a representative velocity in swirl flow. Therefore, the mean velocity, $\bar{U}$, and the turbulence intensity, u', were used as representative characteristics of the turbulent swirl in cylinder.

Figure 13 shows the correlations between $\bar{U}$ and u'. Near TDC of first compression stroke after valve close, N1, the relative intensity of turbulence, $u'/\bar{U}$, is about 0.095 (9.5%), and near TDC of 2nd-5th stroke(N2-N5), $u'/\bar{U}$ is about 0.04-0.06 (4-6%). Although this result was obtained from the data for the case of ε=3.2, the similar results were obtained in other conditions of compression ratio.

Table 2 Swirl ratio, SR, mean velocity, $\bar{U}$, and turbulence intensity, u'

ε	n (rpm)		N1	N2	N3	N4	N5
3.2	600	SR	2.21	1.52	1.17	0.91	0.78
		$\bar{U}$ (m/s)	3.56	2.79	2.05	1.72	1.31
		u'(m/s)	0.323	0.130	0.082	0.066	0.054
3.2	900	SR	2.28	1.59	1.22	1.03	0.89
		$\bar{U}$ (m/s)	5.54	4.14	3.13	2.84	2.33
		u'(m/s)	0.493	0.237	0.199	0.154	0.150
3.2	1200	SR	2.15	1.56	1.28	1.07	0.91
		$\bar{U}$ (m/s)	7.06	5.46	4.10	3.70	3.05
		u'(m/s)	0.731	0.284	0.225	0.214	0.173
4.0	600	SR	2.26	1.47	1.09	0.88	0.68
		$\bar{U}$ (m/s)	3.76	2.42	1.89	1.53	1.31
		u'(m/s)	0.343	0.145	0.129	0.083	0.083
4.0	1200	SR	2.41	1.61	1.24	1.05	0.85
		$\bar{U}$ (m/s)	8.89	6.19	4.60	3.96	3.27
		u'(m/s)	0.795	0.401	0.367	0.302	0.274
4.8	600	SR	2.70	1.92	1.27	0.95	0.77
		$\bar{U}$ (m/s)	4.45	3.22	2.16	1.61	1.32
		u'(m/s)	0.422	0.175	0.130	0.089	0.079
4.8	1200	SR	2.23	1.48	1.10	0.85	0.68
		$\bar{U}$ (m/s)	7.56	5.02	3.71	2.89	2.34
		u'(m/s)	0.730	0.403	0.238	0.203	0.174

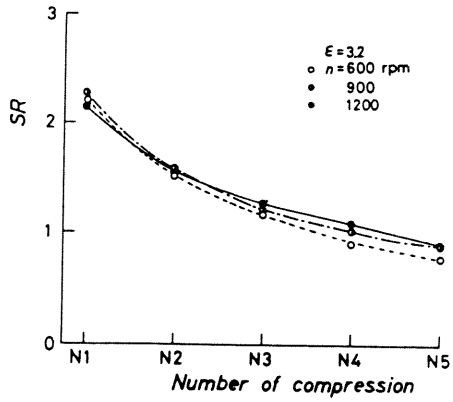

Fig.11 Reduction of swirl ratio (ε = 3.2)

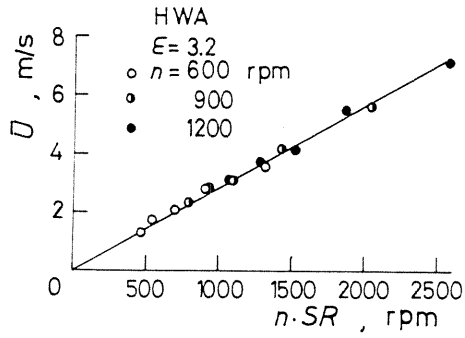

Fig.12 Relation between $\bar{U}$ and n·SR

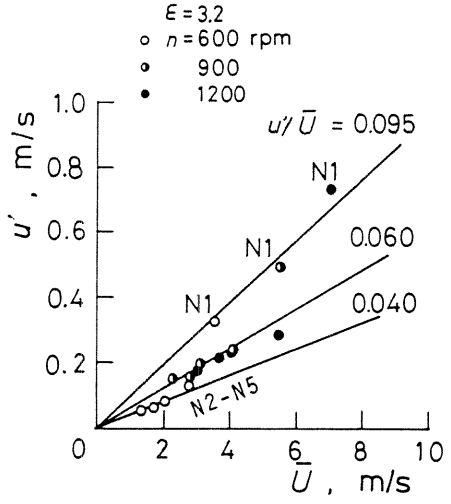

Fig.13 Relation between $\bar{U}$ and u'

Stoichiometric propane-air mixture (equivalence ratio, ϕ=1.0) was ignited by a spark for the several cases of compression ratio, ε, engine speed, n, and swirl ratio, SR. Pressure measurements were made by using a strain gauge type transducer. The pressure diagrams were analyzed thermodynamically and burn rate, burn duration, etc. were obtained. The effects of swirl and turbulence intensity on mass fraction burned, burn rate and burn duration were investigated.

In Fig.14, examples of pressure-volume diagram are shown. Pressure measurements were made

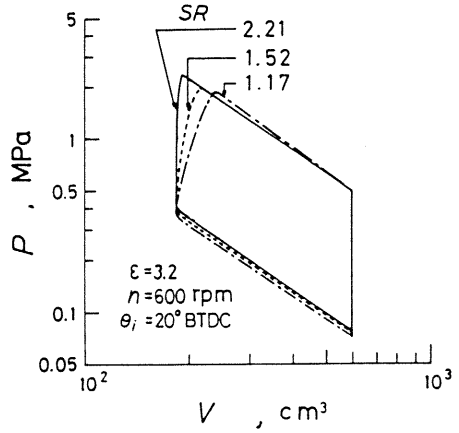

Fig.14 Comparison of pressure-volume diagrams for three different swirl ratios

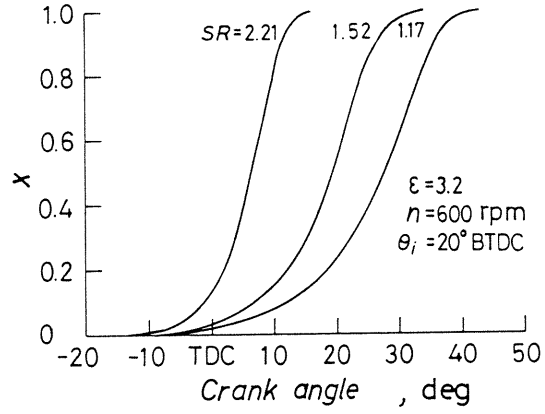

Fig.15 Comparison of mass fraction burned for three different swirl ratios

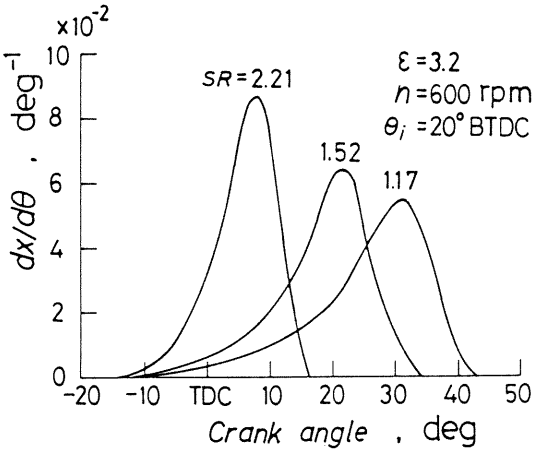

Fig.16 Comparison of burn rate for three different swirl ratios

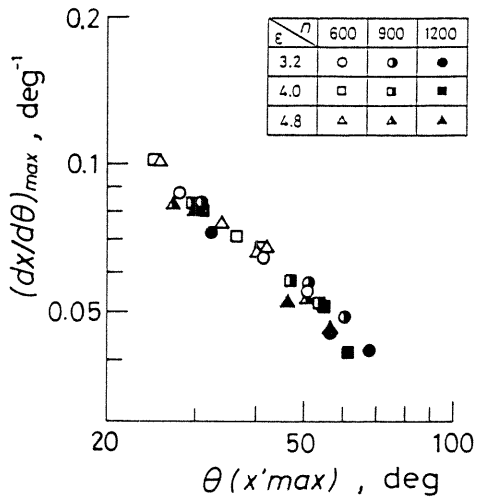

Fig.17 Relation between (dx/dθ)max and θ(x'max)

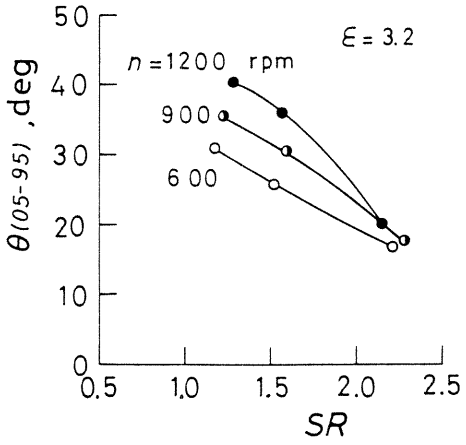

Fig.18 Relation between θ(05-95) and SR (ε = 3.2)

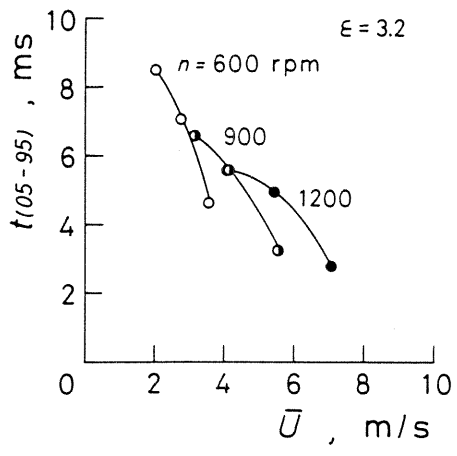

Fig.19 Relation between t(05-95) and $\bar{U}$ (ε = 3.2)

under the conditions that compression ratio, ε, is 3.2, engine speed, n, is 600 rpm, ignition timing, θ_i is 20 BTDC, and that values of swirl ratio near TDC of first, second and third compression stroke (N1,N2,N3) were 2.21, 1.52 and 1.17, respectively.

As shown in Figs.15 and 16, mass fraction burned, x, and burn rate, dx/dθ, were determined from the pressure diagram (Appendix B). They were obtained by a similar method of Lavoie,et al.(14), and the heat loss was estimated by using a heat transfer coefficient presented by Eichelberg(15).

From the results shown in Figs. 14-16, it can be clearly understood that the swirl flow has an important effect on the engine combustion. According to the increase of swirl ratio, the burn duration decreased and the maximun value of burn rate increased. The maximum value of burn rate, (dx/dθ)max, and the crank angle from the spark initiation to the time when (dx/dθ)max occurred, θ(x'max), were investigated for all the cases of experiments. As shown in Fig.17, a good correlation between (dx/dθ)max and θ(x'max) was obtained independent of the engine speed, the compression ratio and the swirl ratio.

The total period from spark initiation (x=0) to completion of the combustion (x=1) were divided to three stages; namely, the initial, main and final stage of combustion were defined as 0-5%, 5-95% and 95-100% burn duration, respectively.

The effect of swirl on the duration of main stage of the combustion was investigated. The results are shown in Figs.18-21. In these figures, 5-95% burn duration is denoted with θ(05-95) in crank angle degrees and t(05-95) in milliseconds. As shown in Figs.18 and 19, 5-95% burn duration was diminished as swirl ratio,

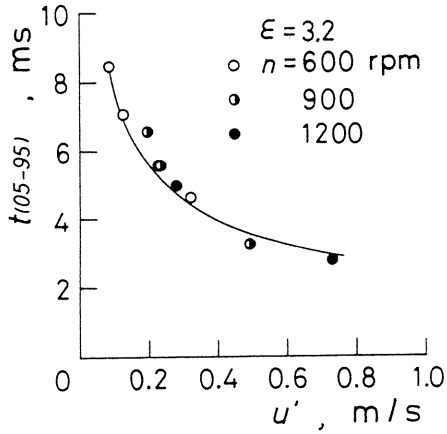

Fig.20 Relation between t(05-95) and u' (ε = 3.2)

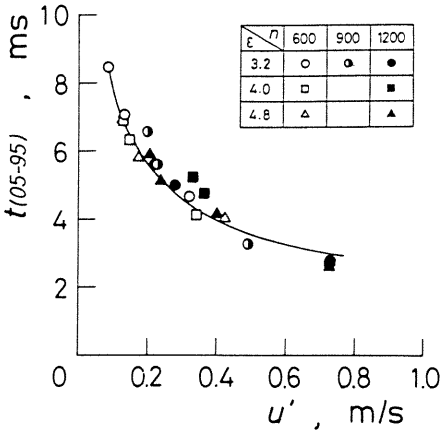

Fig.21 Relation between t(05-95) and u'

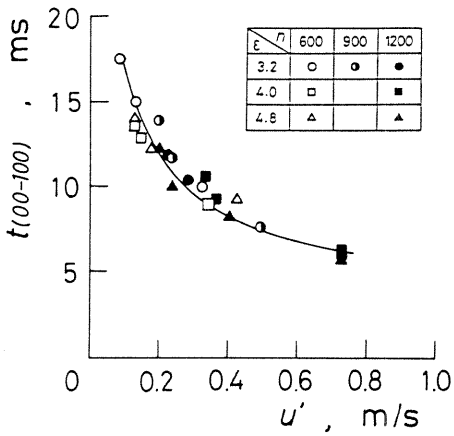

Fig.22 Relation between t(00-100) and u'

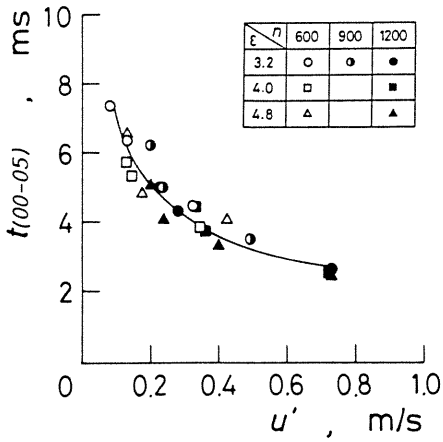

Fig.23 Relation between t(00-05) and u'

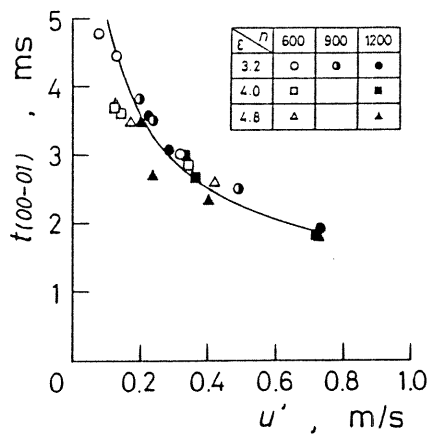

Fig.24 Relation between t(00-01) and u'

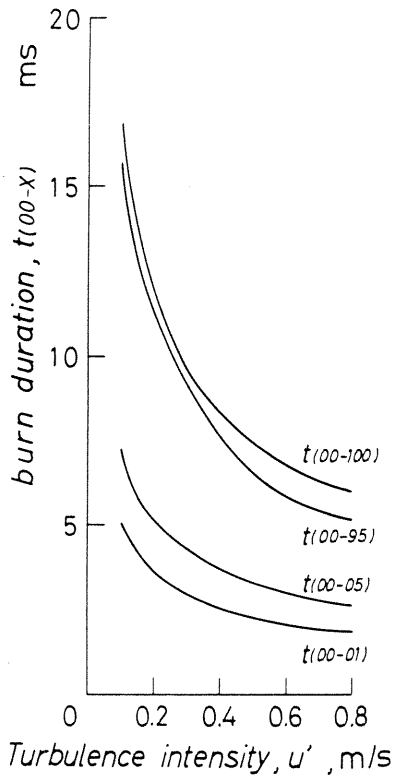

Fig.25 Relation between burn duration and turbulence intensity

SR, and mean velocity, $\bar{U}$, increased. Here, $\bar{U}$ denotes the mean velocity determined at r= 30 mm. The correlations between θ(05-95) snd SR and between t(05-95) and $\bar{U}$ were affected by the engine speed. On the other hand, as shown in Fig.20, a good correlation between t(05-95) and u' was obtained independent of the engine speed and the swirl ratio. Here, u' denotes the intensity of turbulence determined at r=30 mm. Moreover, it has a similar relation for various compression ratio (ε=3.2, 4.0, 4.8), as shown in Fig.21.

Next, the effect of turbulence intensity on the 0-100% burn duration, t(00-100), the 0-5% burn duration, t(00-05), and 0-1% burn duration, t(00-01),are shown in Figs.22-24. The durations in initial and main stages of combustion much depend on turbulence intensity. Effects of engine speed and swirl ratio are not explicit and are included implicitly in the term of turbulence intensity.

The experimental results in burn durations are summarized and illustrated in Fig.25. The burn duration in milliseconds is expressed as a function of u'. The 0-1%, 0-5%, 0-95%, 5-95%, 0-100% burn duration and the ratios of burn durations are expressed by following empirical equations.

$$t(00\text{-}01) = 1.60 / \sqrt{u'} \quad ,$$

$$t(00\text{-}05) = 2.30 / \sqrt{u'} \quad ,$$

$$t(00\text{-}95) = 4.79 / \sqrt{u'} \quad ,$$

$$t(05\text{-}95) = 2.49 / \sqrt{u'} \quad ,$$

$$t(00\text{-}100) = 5.26 / \sqrt{u'} \quad ,$$

$$t(05\text{-}95)/t(00\text{-}100) \fallingdotseq 0.47 \quad ,$$

$$t(00\text{-}05)/t(05\text{-}95) \fallingdotseq 0.92 \quad .$$

The reciprocal of the burn duration expresses the mean value of burn rate in the duration. From the results mentioned above, the mean burning rate can be expressed by the turbulence intensity, u', defined in this study, and can be expressed as a function of u'. The engine speed and the swirl ratio are not included explicitly in the function. The ratio of two values of burn duration is constant. Moreover, as shown in Fig.26, there is a good correlation between maximum burn rate, (dx/dt)max, and turbulence intensity, u'.

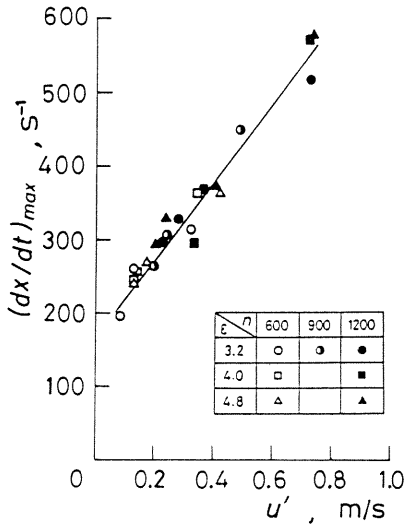

Fig.26 Relation between (dx/dt)max and u'

CONCLUSIONS

By using a specially designed spark-ignition engine with a pancake type combustion chamber, the effect of turbulent swirl on the combustion of stoichiometric propane-air mixture was investigated in various conditions of engine speed and compression ratio.

Swirl flow and its turbulence in cylinder were examined for the case with non-combustion by using three kinds of methods, i.e. smoke-wire method, hot-wire anemometry and laser Doppler anemometry. These results coincided with each other, and the certainty in velocity measurements was comfirmed.

The burn duration and the maximum burn rate were expressed as a function of the turbulence intensity, u', near TDC. The engine speed, n, and the swirl ratio, SR, were not included explicitly in this function. Here, the intensity of turbulence, u', does not include the fluctuating component having lower frequency than about 116 Hz.

This work was supported by a Grant-in-Aid for Special Project Research (No.58116008 in 1983 and No.59110007 in 1984) from the Ministry of Education, Science and Culture of Japan.

REFERENCES

(1) Tabaczynsky, R. J., " Turbulence and Turbulent Combustion in Spark-Ignition Engines ", Prog. Energy Combust. Sci., Vol.2 , pp.143-165, 1976.
(2) Poulos, S.G. and Heywood, J. B., " The Effect of Chamber Geometry on Spark-Ignition Engine Combustion ", SAE Trans., Vol.92, Sect.1, Paper No. 830334, pp.1106-1129, 1983.
(3) Witze,P.O., Martin,J.K. and Borgnakke, C., " Measurements and Predictions of the Precombustion Fluid Motion and Combustion Rates in a Spark Ignition Engine ", SAE Trans., Vol.92, Sect.4, Paper No.831697, pp.786-796, 1983.
(4) Blizard,N.C. and Keck,J.C., " Experimental and Theoretical Investigation of Turbulent Burning Model for Internal Combustion Engines," SAE Trans., Vol.83, Sect.1, Paper No.740191, pp.846-864, 1974.
(5) Tabaczynski, R. J., Ferguson, C. R. and Radhakrishnan, K., " A Turbulent Entrainment Model for Spark-Ignition Engine Combustion," SAE Trans., Vol.86, Sect.3, Paper No.770647, pp.2414-2432, 1977.
(6) Hires,S.D., Tabaczynski, R.J. and Novak, J.M., " The Prediction of Ignition Delay and Combustion Intervals for a Homogeneous Charge, Spark Ignition Engine," SAE Trans., Vol.87, Sect.2, Paper No. 780232, pp.1053-1067, 1978.
(7) Tabaczynski, R.J., Trinker,F.H. and Shannon,B. A.S., " Further Refinement and Validation of a Turbulent Flame Propagation Model for Spark-Ignition Engines," Combust. Flame, Vol.3, pp.111-121, 1980.
(8) Hamamoto, Y., Hashimoto, M. and Ohigashi, S., "Visualization of Air Flow in Cylinder of Internal Combustion Engine by means of Smoke-Wire Method, " Bull. Marine Eng. Soc. Jpn., Vol.7, No.2, pp.173-180, 1976-6.
(9) Wakisaka, T., Hamamoto, Y. and Ohnishi, M., " Measurement of Gas Flow Direction in Combustion Chamber of I.C. Engine -- Application of Spark Tuft Method --," Trans. Soc. Autom. Eng. Jpn., (in Japanese), No.25, pp.44-52, 1982-12.
(10) Hamamoto, Y., Wakisaka, T. and Ohnishi, M.,

" Hot-Wire Anemometry in the Engine Cylinder, " J. Marine Eng. Soc. Jpn., (in Japanese), Vol.16, No.5, pp.455-463, 1981-5.
(11) Wakisaka, T., Hamamoto,T. and Kinoshita, S., "Turbulence Characteristics in Internal Combustion Engines, " Bull. Jpn. Soc. Mech. Eng., Vol.26, No.212, pp.254-261, 1983-2.
(12) Hino, M., "Spectrum Analysis," (in Japanese), p.180, Asakura, 1981.
(13) Hamamoto, Y., Ohkawa, H., Yamamoto, H. and Sugahara, R., " Effects of Turbulence on Combus tion of Homogeneous Mixture of Fuel and Air in Closed Vessel, " Bull. Jpn. Soc. Mech. Eng., Vol.27, No.226, pp.756-762, 1984-4.
(14) Lavoie, G. A., Heywood,J. B. and Keck, J. C., " Experimental and Theoretical Study of Nitric Oxide Formation in Internal Combustion Engines," Combust. Sci. Technol., Vol.1, pp.313-326, 1970.
(15) Nagao, F., " Lecture on Internal Combustion engine," (in Japanese), Vol.1, p.41, Yokendo, 1977.

APPEDIX A

By using the calibration constants of HWA obtained under the atmospheric condition, the equation of the velocity, U, is expressed as follows:

$$\sqrt{U} = \{(I^2 - \frac{Q_E}{r_w}) \frac{\lambda_{go}}{\lambda_g} \frac{T_m - T_{go}}{T_m - T_g} (\frac{T_f}{T_{fo}} \frac{T_{go}}{T_g})^{-0.17} - (I_{*o}^2 - \frac{Q_{Eo}}{r_w})\} \sqrt{\frac{\mu_g \rho_{go}}{\mu_{go} \rho_g}} / B' ,$$

where

$$Q_E = \frac{\pi d_w^2}{2} \lambda_w C_2 (C_1 - T_H) \tanh(\frac{C_2 l_w}{2}) ,$$

$$T_m = \frac{2(T_H - C_1)}{C_2 l_w} \tanh(\frac{C_2 l_w}{2}) + C_1 ,$$

$$C_1 = \frac{\pi d_w l_w h\, T_g + I^2 r_{wo}(1 - \alpha_w T_{mo})}{\pi d_w l_w h - I^2 r_{wo} \alpha_w} ,$$

$$C_2 = \sqrt{\frac{4}{\lambda_w d_w}(h - \frac{I^2 r_{wo} \alpha_w}{\pi d_w l_w^2})} ,$$

The nomenclatures are as follows.

- B' = calibration constant,
- d_w = diameter of the wire,
- h = heat-transfer coefficient from the wire to the gas,
- I = electric current through the wire,
- I_{*o} = calibration constant,
- l_w = length of the wire,
- Q_E = conductive heat loss to the wire supports,
- r_w = electric resistance of the wire,
- T_f = mean film temperature defined as $(T_m+T_g)/2$,
- T_g = temperature of the gas,
- T_H = temperature of the wire support,
- T_m = mean temperature of the wire,
- α_w = temperature coefficient of resistance of the wire,
- λ_g = thermal conductivity of the gas,
- λ_w = thermal conductivity of the wire,
- μ_g = dynamic viscosity of the gas,
- ρ_g = density of the gas.

Subscript o indicates the value at atmospheric condition. When a hot-wire is calibrated under an atmospheric condition, the following relation is obtained.

$$I_o^2 - I_{*o}^2 = B'\sqrt{U} ,$$

where I_{*o}^2 is an extrapolated value of I_o^2 at U=0, and B' is a constant.

APPENDIX B

From the state equation for burned gas and unburned gas, and the conservation equation of energy and mass of gas in the cylinder, the mass fraction of burned gas, x, is expressed by the following equation.

$$x = \frac{PV - P_i V_i + Mc_{vu}(\kappa_b - \kappa_u)(Tg_u - Tg_{ui}) + (\kappa_b - 1)(W_\theta + L_\theta)}{M\{(\kappa_b - \kappa_u) c_{vu} Tgu + (\kappa_b - 1) H_u\}} ,$$

where the nomenclatures are as follows.

- c_v = mean specific heat in constant volume,
- H_u = heat of combustion of the mixture of unit mass,
- L_θ = heat loss during crank angle θ after spark initiation,
- M = mass of cylinder charge,
- P = pressure in cylinder,
- T_g = gas temperature,
- V = volume of the cylinder,
- W_θ = work of gas during crank angle θ after spark initiation,
- κ = ratio of specific heats.

Subscripts i, u and b indicate the ignition timing, the unburned gas and the burned gas, respectively. The temperature Tgu was obtained by the equation,

$$T_{gu} = T_{gi} (\frac{P}{P_i})^{(\kappa_u - 1)/\kappa_u} ,$$

where Tgi was calculated from the gas temperature at BDC, Tg_{BDC}, on the basis of polytropic compression. Then, Tg_{BDC} was determined with a fine resistance wire thermometer. Its sensing element was made of tungsten wire having a diameter of 5 μm and a length of 1 mm.

By using a coefficient of heat transfer presented by Eichelberg, the heat loss, L_θ, was obtained from the following equation.

$$L_\theta = \int_{t_i}^{t} K (PT_g)^{1/2} C_m^{1/3} F (T_g - T_w)\, dt ,$$

where C_m = mean piston speed,
F = surface area of the combustion chamber wall,
K = experimental constant,
R = gas constant,
Tg = PV/MR,
Tw = wall temperature,
t = time.